

Reduced Subboundary Misalignment in SOI Films Scanned at Low Velocities

Loren Pfeiffer
K. W. West
D. C. Joy
J. M. Gibson
A. E. Gelman*

AT&T Bell Laboratories
Murray Hill, New Jersey 07974

ABSTRACT

Silicon-on-Insulator (SOI) films on SiO₂ scan-melted at low velocities (20 to 300 $\mu\text{m}/\text{sec}$) with reduced thermal gradients at the melt-freezing interface are found to have qualitatively different properties from similar films melt-scanned at higher gradients and scan velocities. The transition between the two regimes appears to be abrupt. Scanning at intermediate velocities often results an admixture of patches containing one or the other type of material. The slow scan regime is characterized by long straight non-branched subboundaries having a lateral spacing 50-60 μm , and very small tilt misalignments of 0.1° or less. These slow scan subboundaries are found to consist largely of threading dislocations in contrast conventional subboundaries which are tilt boundaries of up to 3° and typically consist of edge dislocations running in the plane of the film.

We recently reported preliminary experiments¹ that show that scanned zone melting of amorphous silicon-on-insulator (SOI) structures at very low velocities results in SOI films with markedly improved properties. Here we report new experiments which suggest that low velocity scanned melting must be accompanied by a reduced thermal gradient at the growth interface. The two conditions together lead to SOI recrystallization of a new type that is characterized by material qualitatively unlike that grown using faster scans and higher gradients.

A clear example of the contrast between the slow scan and the conventional material is illustrated in Fig. 1. Here a 1.3 μm amorphous Si film deposited on 1 μm of thermally grown SiO₂ and capped with 2 μm of deposited SiO₂ and then by 300Å of sputter deposited Si₃N_{1.5} was recrystallized using our graphite strip heater apparatus^{2,3} set at 1210°C wafer base temperature, 2100°C upper heater and 30 $\mu\text{m}/\text{sec}$ scan velocity. Near the left edge of the microphoto the upper heater was abruptly turned off resulting in a locally faster scan of the freezing interface. Removal of the cap oxide and a Schimmel defect etch⁴ shows that the slowly scanned material has faintly defined subboundaries that are resistant to the defect etch. However in the area near where the wire was turned off, the effectively faster scan resulted in normal recrystallization subboundaries that are deeply etched by the defect etch.

* Present address: Department of Physics, Massachusetts Institute of Technology, Cambridge, Mass.

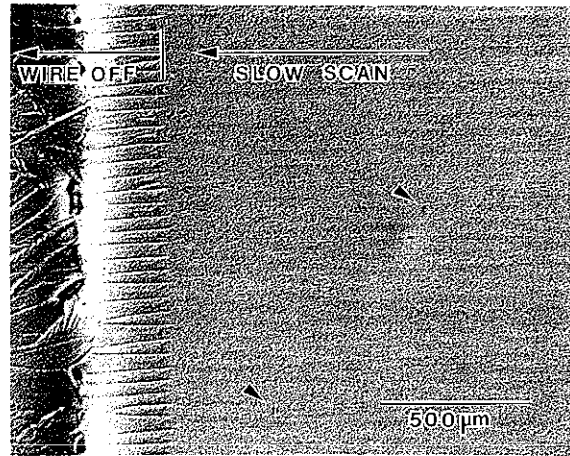


Fig. 1 Defect etched SOI film melt-recrystallized using a $30 \mu\text{m}/\text{sec}$ scan. Near the left edge of the microphoto the upper graphite strip heater wire was abruptly turned off effectively increasing the scan velocity under the wire as it cooled. Note the comparatively deep etching of the subboundaries in this region.

In Fig. 2 the slow and fast SOI growth regimes are compared using a scanning electron microscope (SEM) in the electron backscatter mode to form electron channeling images. The major portion of the figure is an electron channeling image of a $\sim 1 \text{ mm}^2$ area of the slow scan SOI sample of Fig. 1. The inset of Fig. 2 is a comparable backscatter channeling image at the same magnification from a similar SOI structure, conventionally melt-scanned at $1.5 \text{ mm}/\text{sec}$ with a thermal gradient several times larger at the growth interface. The slow growth material is seen to contain fewer but many times larger area subgrains. In addition there is little channeling contrast between adjacent slow growth subgrains indicating a much closer alignment of the crystallographic texture than the conventional SOI material of the inset. Notice also that the slow growth subboundaries are straight and unbranched, in sharp contrast to the highly branched interactive behavior characteristic of conventional material.

In Figs. 3 and 4 the slow and fast growth regimes are again compared; this time by using the SEM for diffraction channeling⁵ in a mode known as ECP or Electron Channeling Pattern. This is perhaps the most powerful method of characterizing subgrain crystallography in an SOI sample. It allows a simultaneous measure of the crystallographic alignment for each of many subgrains in a large area. To do ECP one selects an area on the sample to be imaged, and then by activating ramping circuits in the SEM the electron beam is caused to rock over a solid angle of several degrees about its usual normal incidence axis, all the while preserving the focused spot of the original region chosen on the sample. If the area chosen for imaging is a single crystal of for example (100) Si, rocking the

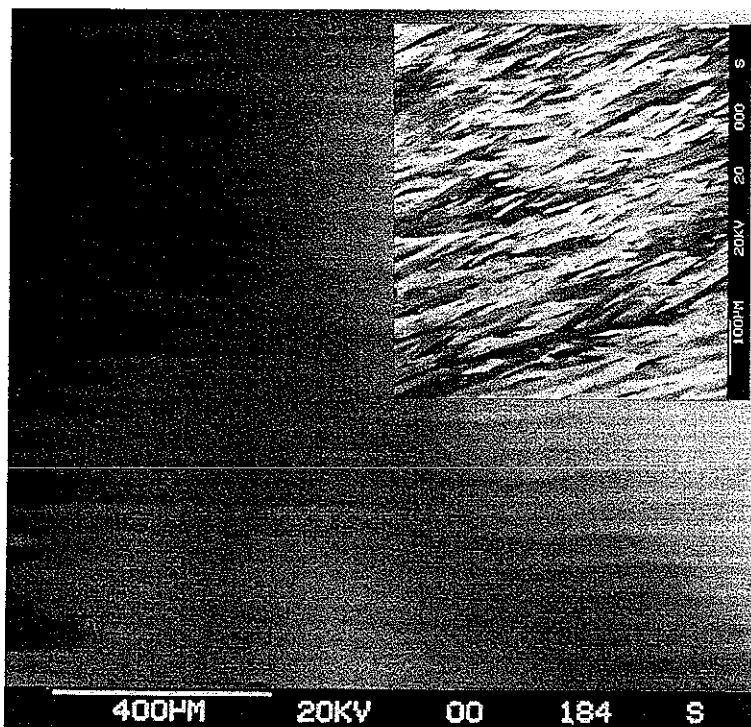


Fig. 2 Channeling contrast comparison of slow and fast SOI recrystallization using an SEM in the electron backscatter mode. The material in the inset was scan melted at 1.5 mm/sec; the main figure is of material scanned at 30 $\mu\text{m}/\text{sec}$. The scale is the same for both parts of the figure.

electron beam through the various nearby Bragg planes produces contrast by electron diffraction channeling and results in the Si(100) ECP signature pattern shown in Fig. 4.

Figure 4 was obtained by rastered rocking of the SEM beam through a solid cone of about 6° semiangle while focused to a $40 \mu\text{m}$ dia. spot on a single subgrain of the slow-scan sample of Fig. 1. Because this pattern is in fact indistinguishable from a pattern taken from a virgin Si(100) wafer, we conclude the slow-scan SOI material is structurally ideal within each subgrain by this test.

By moving the crossover point of the SEM beam rocking-cone to a plane somewhat in front of the sample a substantially larger area can be imaged. Fig. 3a shows the resulting ECP image for a larger area of the slow-growth material of Fig. 1. It is effectively a real space image of the sample built up by a superposition of channeling diffraction patterns that change locally if and only if the crystallography of the sample locally changes. The marker arrows on Figs. 1 and

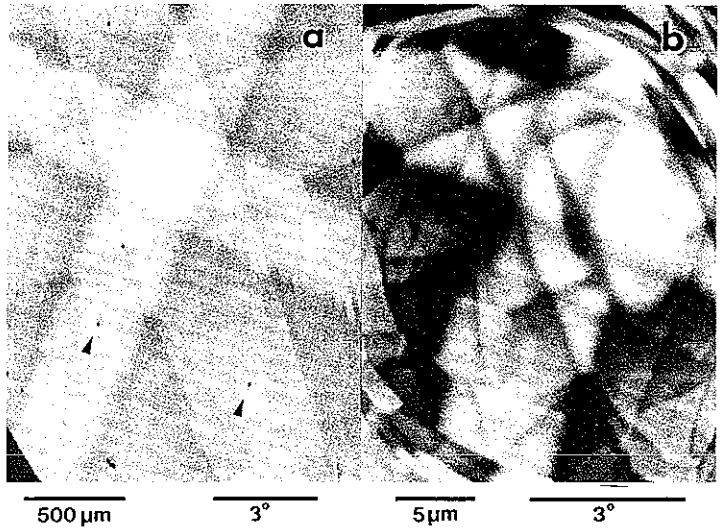


Fig. 3 Electron channeling diffraction comparison of slow, (3a) and fast, (3b) SOI recrystallization using an SEM in ECP mode. Note the effective area sampled is more than 3000 times larger for the slow scan material on the left.

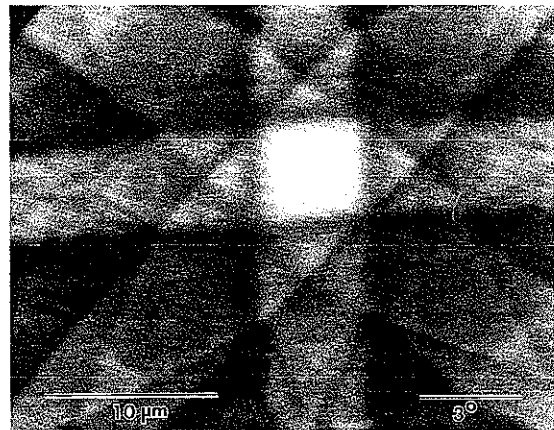


Fig. 4 Electron channeling diffraction pattern from a 40 μm diameter region of interest of the slow scan material. This pattern is indistinguishable from those obtained from ideal (100) silicon wafers.

3a point to a pair of defects on the slow-growth sample separated by 0.82 μm . The diffraction pattern of Fig. 3a arises thus from an area on the slow-scan sample exceeding 1.5 mm by 2.5 mm and includes more than 30 subgrains. The slight tilt misalignments between these subgrains⁶ show up in the figure as 0.1° jogs in the 2.6° wide Si <220> diffraction strips.

Figure 3a is intended to be contrasted with 3b, which is a 40 μm dia. selected area ECP obtained from the conventionally melt-scanned SOI material shown in the inset of Fig. 2. Because the tilt misalignments between the many small subgrains in this material are a degree or more it is not possible to image over a larger selected area without entirely losing the ECP diffraction image in a chaotic jumble of misaligned subgrains. Figure 3 thus summarizes two useful points. It provides a measure of the significant improvement⁶ in crystallographic quality accomplished by slow growth scan melting. And it emphasizes the importance of explicitly specifying for ECP data the size of the effective real space image and perhaps also the conical angle through which the SEM beam was rocked.

Transmission electron microscopy (TEM) studies in plan view of SOI crystal growth in the slow and fast regimes are compared in Fig. 5. On the right in fig. 5b we show the initiation of a conventional subboundary in a 4000Å silicon film that was melt-crystallized using a scan velocity of 1.5 mm/sec. The figure shows an initial tangle of dislocations and then four parallel dislocations aligned along the scan, in agreement with earlier studies by Pinizzotto,⁷ and then by Baumgart and Phillip,⁸ who showed that conventional melt-recrystallization subboundaries in SOI films typically consist of parallel arrays of edge dislocations lying in the plane of the film along the growth direction.

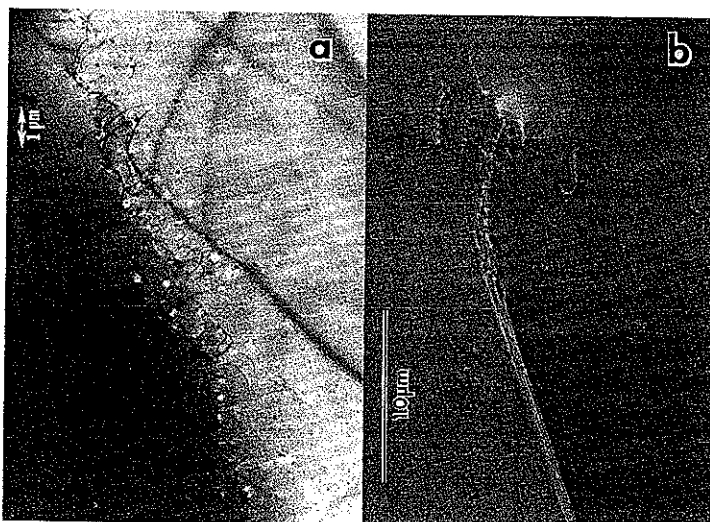


Fig. 5 Plan view TEM comparison of subboundaries in the slow, (5a) and fast, (5b) melt-scanned SOI material.

TEM images of slow-scan subboundaries on the other hand usually contain no dislocations running along the scan in the plane of the film. Figure 5a shows a typical slow-scan subboundary from the melt-recrystallized film of Fig. 1. The dislocations in this plan view TEM micrograph are all short and thread through the thickness of the silicon film from the buried oxide to the capping oxide. The ECP data suggests they have predominantly screw character. Subboundaries consisting exclusively of these so-called threading dislocations give the slow-scan SOI material an entirely different character from the material recrystallized at faster scan rates.

Figure 6 is a plan view TEM micrograph of a another subboundary in the slow scan material, that shows somewhat unusual behavior. This sample was chemically defect etched (as was the material of Fig. 5a) before the TEM specimen was prepared. In Fig. 6 the defect etch appears to have highlighted a trail of impurities running approximately parallel to, but several microns to the side of, the threading dislocations making up the slow scan subboundary. This sort of behavior is not unexpected in terms of the model of a faceted freezing crystal growth front.^{9,10} From the point of view of that model one would expect that impurities in the melt would be rejected by the (111) , $(\bar{1}\bar{1}\bar{1})$ facets of the growing single crystal solid and would collect just ahead of the interior corners formed by these facets. At a sufficient concentration the impurities would become entrapped in the solid forming a series of trails coincident with the expected subboundaries that also form at these interior corners. However, since the impurity rejection and trapping mechanisms are subject to local fluctuations, it is not unreasonable that occasionally there develops a lateral offset between a subboundary and the impurity trail that formed with it.



Fig. 6 TEM plan view of a slow scan subboundary showing a lateral offset between a row of threading dislocations and a row of impurity precipitates.

We believe that the structural characterizations just summarized support the claim that the slow scan SOI material is qualitatively different from the usual melt-recrystallized material regrown at scan rates several times faster. Moreover we can find no evidence for a gradual transition between the two growth regimes. Scan melting using a gradual thermal gradient at the melt-freezing interface results in large uniform areas of slow growth SOI material if the scan velocity is between 15 and 100 $\mu\text{m}/\text{sec}$. At higher scan velocities to about 300 $\mu\text{m}/\text{sec}$ we obtain either fast growth material or an admixture of patches containing either one or the other type of material.

In addition to a reduced scan velocity slow growth recrystallization also appears to require the introduction of a reduced thermal gradient at the melt-freezing interface. The two requirements tend to interact in a strip heater experiment; a reduction in scan velocity tends to increase the thermal gradient at the growth interface unless other compensating changes are made. However, if the scan velocity is held constant it is possible to independently vary the thermal gradient by controlling the width of the melted zone through the temperature of the upper strip heater. This is easily seen with the help of Fig. 7, which for a 1.5 mm/sec scan shows the calculated temperature of the SOI film as a function of lateral distance away from our upper heater for two wire temperatures. Referring again to the faceted melt-freezing interface model^{9,10} we recall that a given scan velocity

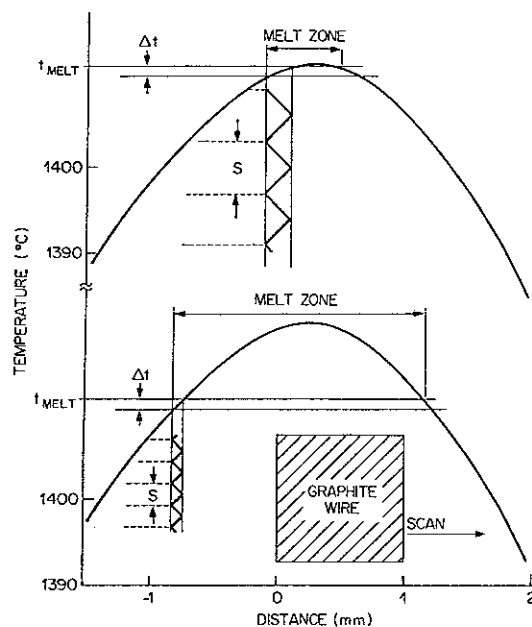


Fig. 7 Relation of the expected thermal gradient at the freezing interface to the width of the melt zone.

implies a corresponding maximum undercooling ΔT , which from Fig. 7 establishes the spacing of adjacent interior corners of the faceted freezing front, and thus the lateral spacing s between the subboundaries in the material.¹¹

Figure 8 shows experimental results that clearly confirm these ideas. For this experiment a 1 mm by 1 mm graphite wire was scanned at a constant velocity of 1.5 mm/sec across a 100 mm dia SOI wafer using a wafer to wire clearance of 1 mm. The SOI structure was a 0.5 μm amorphous Si film deposited over 1 μm of thermal SiO_2 and capped with 2.5 μm of deposited SiO_2 and 300 \AA of sputtered $\text{Si}_3\text{N}_{1.5}$. The only variable in the experiment was the temperature of the upper graphite wire, which was increased in steps of about 50°C from 2200°C to 2500°C after allowing about 2 cm of scanned SOI recrystallization at each temperature step. Removal of the cap oxide and a Si defect etch⁴ revealed the remarkable systematic changes in the subboundary networks shown in Fig. 8. In agreement with the faceted crystallization front model and the argument of Fig. 7, we find the average lateral spacing \bar{s} between subboundaries decreases by nearly a factor of four¹¹ as the melt width increases due to the stepped increases in temperature of the upper heater.

We believe this dependence of \bar{s} on thermal gradient is the dominant effect in many previous experiments on subboundary spacing. In particular it appears to

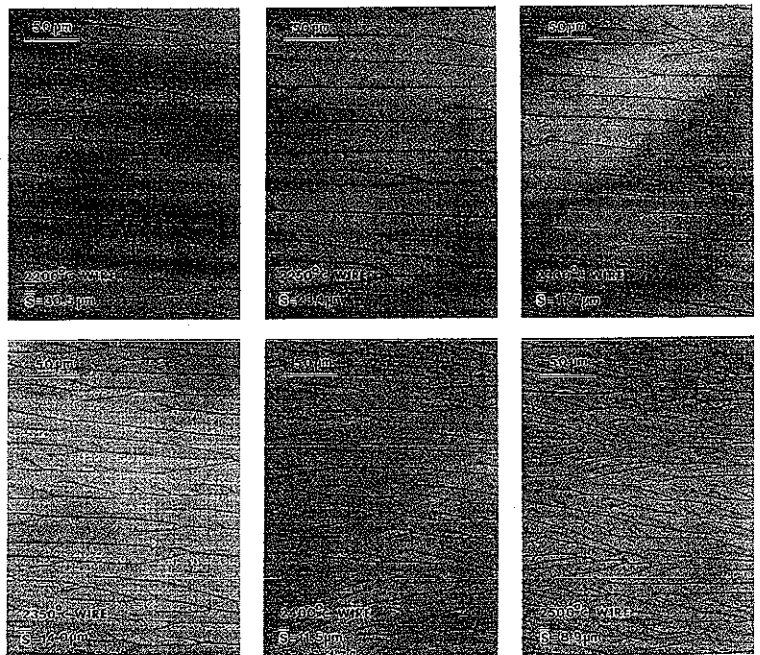


Fig. 8 Lateral spacing of SOI subboundaries as a function of the temperature of the upper heater wire. All microphotos were taken from the same wafer scanned at a constant velocity of 1.5 mm/sec.

account for the proportionately between \bar{s} and the square root of the scan speed that has been studied both experimentally^{12,10} and by computer modeling.¹⁰ The argument goes as follows: An increase in scan velocity tends to smear out the trailing slope of the temperature profile in the silicon film because there is less time for radiative cooling at any given distance from the receding graphite wire. This effectively reduces the thermal gradient at the growth interface which by the argument of Fig. 7 increases the size of the growth facets and thus the lateral spacing of the subboundaries.

An implication of this line of reasoning would be to try to scan at high velocity using a narrow melt width, as this might be expected to increase the subboundary spacing by both effects. This idea fails for the practical reason that the above conditions do not allow enough time to establish complete melting of the amorphous silicon. On the other hand a very slow scan allows complete melting even if one chooses a very narrow melt width. This makes it possible to establish an exquisitely small thermal gradient at the growth interface during low velocity scans. It is this we believe that accounts for the otherwise unexpectedly wide lateral spacing of the subboundaries in the slow-scan material.

The experiment of Fig. 8 has even more to say about the role of thermal gradients during scanned zone melting. For each of the melt scans in that

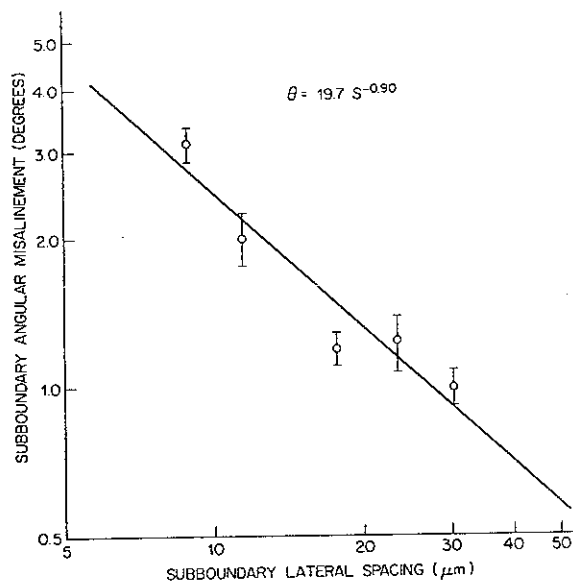


Fig. 9 Measured average crystallographic angular misalignment $\bar{\theta}$ for a number of subboundaries as a function of the average lateral spacing \bar{s} of those subboundaries as obtained from the experiment of Fig. 8.

experiment the average change in crystallographic alignment $\bar{\theta}$ at a number of subboundaries was measured using an SEM in the ECP mode. The results are plotted as Fig. 9. We find the quite unexpected result that $\bar{\theta}$ is proportional to the reciprocal of \bar{s} . This says that total crystallographic disorder in these samples is not conserved, as might be expected from subboundary formation models based on the incorporation of melt impurities. It shows instead that low thermal gradients can reduce the total crystallographic disorder in a SOI film both by increasing the lateral separation between subboundaries and also by reducing the angular misalignment between subgrains at each subboundary. Additional implications of this experiment are discussed in the paper by Gibson, Pfeiffer, West and Joy in this proceedings.

1. L. Pfeiffer, K. W. West, S. Paine and D. C. Joy, *Mat. Res. Soc. Symp. Proc.* **35**, 583-592 (1985).
2. L. Pfeiffer, G. K. Celler, T. Kovacs, and McD. Robinson, *Appl. Phys. Letts.* **43**, 1048-1050 (1983).
3. Similar apparatus is described in better detail in the paper by J. C. C. Fan, B-Y Tsauro, R. L. Chapman, and M. W. Geis, *Appl. Phys. Letts.* **41**, 186-188 (1982).
4. D. G. Schimmel, *J. Electrochem. Soc.* **126**, 479 (1979).
5. D. C. Joy, D. E. Newbury and D. L. Davidson, *J. Appl. Phys.* **53**, R81 (1982).
6. Because no subgrain is in this sample crystallographically misaligned by more than 0.1° this slow scan SOI material yields an ideal value of .03 for the Rutherford Backscattering (RBS) channeling to random ratio using 2 MeV ^4He . for further details and an RBS spectrum see Ref. 1.
7. R. F. Pinizzotto, *J. Cryst. Growth* **63**, 559-582 (1983).
8. H. Baumgart and F. Phillipp, *Mat. Res. Soc. Symp. Proc.* **35**, 593-598 (1985).
9. M. W. Geis, H. I. Smith, D. J. Silversmith, R. W. Mountain and C. V. Thompson, *J. Electrochem. Soc.* **130**, 1178 (1983).
10. L. Pfeiffer, S. Paine, G. H. Gilmer, W. van Saarloos and K. W. West; *Phys. Rev. Letts.* **54**, 1944-1947 (1985).
11. The first report of scanned melting experiment showing the relationship between subboundary spacing and thermal gradient may be found in Ref. 9. In that work two upper heater wires were used to produce a shallower temperature gradient.
12. M. W. Geis, H. I. Smith, B-Y Tsauro, J. C. C. Fan, D. J. Silversmith and R. W. Mountain, *J. Electrochem. Soc.* **129**, 2812 (1982).